Ion Acceleration and Direct Ion Heating in Three-Component Magnetic Reconnection

Y. Ono, M. Yamada,* and T. Akao
Department of Electrical Engineering, University of Tokyo, 7-3-1 Hongo, Bunkyo-Ku, Tokyo 113, Japan

T. Tajima and R. Matsumoto†
Institute for Fusion Studies, The University of Texas at Austin, Austin, Texas 78712-1060
(Received 10 October 1995)

Ion acceleration and direct ion heating in magnetic reconnection were experimentally observed during counterhelicity merging of two plasma toroids. Plasma ions are accelerated up to the order of the Alfvén speed through contraction of reconnected field lines with three components. The significant ion heating (from 10 up to 200 eV) is attributed to direct conversion of magnetic energy into ion thermal energy, in agreement magnetohydrodynamic and macroparticle simulations.

PACS numbers: 52.30.Jb, 96.60.Pb

Magnetic reconnection has been recognized as key physics for topological changes of magnetized plasma configurations. Dynamic reconnection of solar flare is often considered to accelerate plasma particles, leading to the anomalous heating of solar coronas [1]. In the magnetosphere, reconnection at the magnetopause may cause heating of plasma particles. In many theoretical models, such as those of Sweet-Parker and Petschek [2,3], magnetic reconnection is caused by local diffusion of neutral sheet current flowing along the X line. It has been generally conceived that Ohmic dissipation of the current sheet is the main process which transforms the magnetic energy into electron and ion thermal energies, and that it is first transformed to the thermal energy of current-carrying electrons and then to the ion thermal energy through electron-ion collisions. However, the outflow jet associated with reconnection, especially the field-aligned jet, has been discussed as an important energy conversion process in several theories, magnetohydrodynamics (MHD), and test-particle simulations [4–10]. Plasma particle motions such as their $\mathbf{E} \times \mathbf{B}$ drift have also been investigated around the X point, leading to further understanding of the plasma heating process around the field-null region [9,10]. A local X-point structure has been investigated by Stenzel and Gekelman, using a thin electrode discharge-current channel [11], leading to the verification of the 2D plasma flow of reconnection. However, the heating and acceleration characteristics of reconnection, such as the anomalous energy conversion to ions, remain unresolved.

An important question has also been raised as to whether direct ion heating is possible during magnetic reconnection. The ion temperature T_i is often observed to be higher than the electron temperature T_e in some fusion plasmas such as reversed field pinches (RFPs) [12] and spheromaks [13]. Though anomalous ion heating has been widely investigated in terms of the magnetic fluctuations, the multiple reconnection points have prevented further elucidation of its cause and mechanism.

This paper describes the first clear evidence of direct ion heating of single magnetic reconnection, based on a laboratory experiment on toroidal plasma merging. Its interpretation is aided by computer simulations. They have verified important steps of direct ion heating: (1) ion acceleration during reconnection and (2) the resultant energy transfer to the ion thermal energy.

In the present experiment, ion acceleration in the toroidal direction and a large increase in the ion temperature T_i are measured around a single reconnection point. Two merging spheromaks with equal but oppositely directed toroidal magnetic fields B_t are used to produce an axisymmetric "X-point" line. The merging angle of reconnecting field lines is always about 180° [14,15]. The TS-3 merging device [15] is used to produce two spheromaks and to merge them together in the axial direction. Its cylindrical vacuum vessel with diameter 0.8 m and length 0.9 m has two internal poloidal field (PF) coils and two sets of eight-pair electrode rings to produce poloidal and toroidal magnetic fluxes of the two initial spheromaks, respectively. A 2D array of magnetic probes is located on the r-z plane of the vessel to measure 2D contours of poloidal and toroidal magnetic fields on a single discharge. These data are used to calculate poloidal flux contours and magnetic energy evolutions of the merging toroids. The Doppler width of the H_β line and the Doppler shift of the C_{II} line (and H_β line for confirmation) are used to measure radial profiles of T_i and velocity on the midplane. Figures 1(a) and 1(b) show the axial profiles of B_t at $r = 18$ cm and the poloidal flux contours during the reconnection of the two spheromaks with opposite B_t. They have plasma currents of ~30 kA and major and minor radii of 18 and 12 cm, right after their formations (at $t = 10$ μsec). At $t = 17.5$ μsec, two magnetic axes merge completely, indicating that the reconnection time is less than 10 μsec. Note that the B_t profile offers an overshoot or an oscillation after reconnection. Until $t = 17.5$ μsec, the polarity of B_t is still kept as initially given by the two spheromaks: positive on the left-hand side and negative on the right-hand side. Figure 1(c) shows the radial profiles of the global ion velocity V in the toroidal direction measured on the midplane. From $t = 12.5$ to

 0031-9007/96/76(18)/3328(4)$10.00

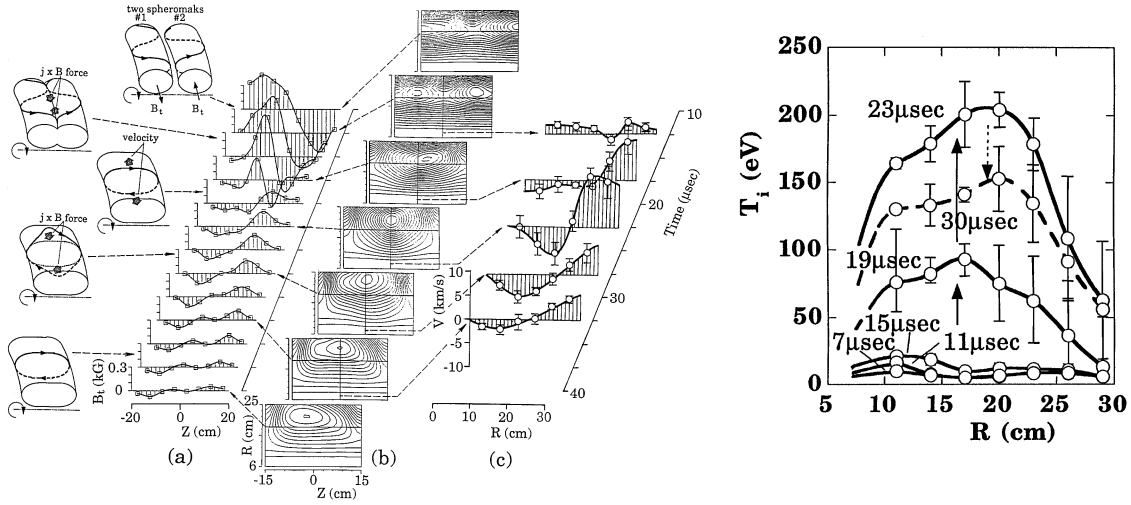

FIG. 1. Axial profiles of the toroidal magnetic field B_t at $r = 18$ cm (a), poloidal flux contours on the r-z plane (b), radial profiles of the ion global velocity V in the toroidal direction on the midplane (c), and radial profiles of ion temperature T_i on the midplane (d) during the reconnection of two merging sphermoks with equal but oppositely direction B_t.

22.5 μsec, V is observed to increase in both edge regions. The largest velocity shear is observed at $t = 22.5$ μsec, that is, ~ 3 μsec after the B_t profile passes the zero line and changes its polarity: negative on the left-hand side and positive on the right-hand side. The ion velocity is positive for $r > 18$ cm and negative for $r < 18$ cm, in agreement with the polarity of the field-line motion observed in Fig. 1(a). Both measurements indicate that the inner halves and outer halves of the reconnected field lines accelerate plasma ions oppositely in the toroidal direction. The maximum $V \sim 12$ km/sec observed at $r = 22$ cm is about 1 to $\frac{1}{3}$ of the field-line velocity ~ 15–45 km/sec that is the order of the local Alfvén speed calculated from $n_i \sim 2 \times 10^{20}\,\mathrm{m}^{-3}$ and $B = 0.1$–0.3 kG. Local ion velocity around the X point is probably larger than the measured globally averaged velocity, because not the local upstream flow but the global downstream flow mostly oriented to the toroidal direction is measured with a resolution of 3 cm in the r and z directions that is comparable to or larger than the width of the compressed current sheet. The velocity shear is observed to gradually vanish after $t = 22.5$ μsec. The B_t field with reversed polarity also starts decreasing after $t = 25$ μsec, suggesting that the oppositely directed field-line motion decreases the ion velocity. This overshoot or oscillation of the reconnected field lines is observed at most once or rarely twice. Finally, the B_t profile relaxes uniformly to zero at $t = 40$ μsec, indicating the formation of a field-reversed configuration (FRC) [16].

The acceleration of plasma ions is connected with a large increase in T_i. Figure 1(d) shows the radial profiles of T_i measured on the midplane. In the initial reconnection phase (at $t = 11$ μsec), T_i is uniformly small, ~ 10 eV. Right after reconnection, T_i starts increasing rapidly at $t = 15$ μsec and reaches a peak value as large as 200 eV at $t = 23$ μsec. Around this time, the velocity shear also reaches its maximum amplitude during the first overshoot of the reconnected field lines. As shown in Fig. 1(d), the magnetic reconnection significantly increases the ion thermal and kinetic energies, producing the macroscopic reconnection outflow observed in Fig. 1. With the help of large ion viscosity in the field-annihilated region, the overshoot motion of field lines possibly contributes to the thermalization process of the ion kinetic energy. The energy flow of our reconnection experiment is illustrated in Fig. 2. Based on the T_i measurement, the total increase in the ion thermal energy $W_{i,\mathrm{th}}$ is $\sim 180 \pm 30$ J. This value is as large as 80% ($\pm 20\%$) of the dissipated magnetic energy $W_m \sim 230 \pm 20$ J (the whole toroidal magnetic energy and part of the poloidal magnetic energy) during reconnection. This fact indicates that W_m is transformed mostly into $W_{i,\mathrm{th}}$. However, the magnetic energy dissipation W_{sheet} of the neutral current sheet is estimated to be as small as 20 J. This value is calculated from the measured 2D magnetic field contours, using $W_{\mathrm{sheet}} \sim 2\pi R \delta L E j \tau_{\mathrm{rec}}$, where R is the radius of the toroidal X-point line, δ and L are

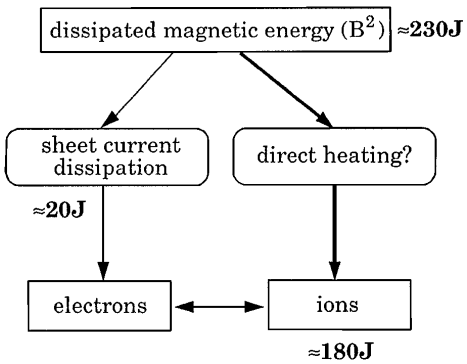

FIG. 2. Energy flow pattern of magnetic reconnection with $\theta \sim 180°$. The magnetic energy is transformed mostly into the ion thermal energy not by the neutral current sheet dissipation but by the direct energy conversion process.

the width and the length of the current sheet, E and j are the toroidal electric field and the toroidal current density at the X point, and $\tau_{\rm rec}$ is the reconnection time [15]. These comparisons lead us to conclude that significant ion heating is caused directly by the slingshot motion in the bulk plasma and not by the dissipation of the neutral sheet current. The direct energy conversion is probably explained by the ion viscosity heating in the process of forming the velocity shear and not by the finally formed global ion flow itself, whose energy is less than 20 J. They can be compared with the following two numerical simulations, which will be described only to the extent to elucidate the above physical phenomenon in this experimental paper.

A 3D MHD simulation of two merging flux tubes with counterhelicity magnetic fields has been carried out using the modified Lax-Wendroff method [17] with artificial viscosity [18]. Ohm's law $\mathbf{E} = -\mathbf{v} \times \mathbf{B} + \eta \mathbf{J}$ is adopted where η is the spatially uniform resistivity parametrized by the magnetic Reynolds number $R_m = 10^3$. The number of grid points used is $(N_r, N_\theta, N_z) = (42, 42, 82)$. The toroidal and poloidal magnetic fields of the flux tubes are $B_t = B_0 J_0(2r/a)$ and $B_p = B_0 J_1(2r/a)$, respectively, where J_0 and J_1 are Bessel functions. As is the case in experiments [14,15], distinct from the cohelicity case, two tubes with counterhelicity merge rapidly on the order of tens of the Alfvén times ($\tau_A = a/v_A$). Figure 3(a) shows the isosurfaces of magnetic field strength (white), isosurfaces of $v_t = \pm 0.3 v_A$ (blue and orange), velocity vectors (green), and magnetic field lines (red) at $t = 86\tau_A$ and at $t = 100\tau_A$. Once the merging starts and the Y points appear, rapid reconnection progresses and the separation of the two Y points quickly enlarges. During this stage, the oppositely directed field lines in the θ-R plane rapidly reconnect, and as they do they are now directed in the z direction (see the magnetic field lines at $t = 86\tau_A$). With this explosive process, the fluid undergoes slingshot motion in the toroidal direction, as seen in the velocity vectors in Fig. 3(a). The maximum velocity of the fluid is $\sim 0.8 v_A$. The velocity isosurface at $t = 86\tau_A$ also shows that the direction of the slingshot velocity changes with R, consistent with the experiment. The magnetic reconnection occurs in the tilted plane with nearly no magnetic field normal to this plane, as shown in the schematic pictures in Fig. 1. Once reconnection occurs on this particular plane, the contraction of the reconnected field lines accelerates the plasma with ellipsoidal cross section in the toroidal direction (with a tilt toward the R direction). By this time, the next action of reconnection of two field lines in the opposite toroidal direction occurs in the inner part of the two Y points that are now rapidly receding. Again the above process repeats itself for the next slice of the plasma. The receding ellipsoidal plasma slice oscillates due to its magnetic tension (primarily Alfvén oscillations), thus causing oscillating B_t and v_t as a result. These results seem to correlate well with what we observe in Fig. 1. Note that the plasma thermal energy increases significantly right after the reconnection. The increment of thermal energy is much larger than the kinetic energy, revealing the direct plasma heating observed in Fig. 1(d).

In the counterhelicity case, there appears a substantial region of null or very weak field, where ions are unmagnetized. It is here that the full description of heating needs kinetic dynamics and also here that significant direct ion momentum transfer and subsequent heating take place. Thus the slingshot oscillations and acceleration or heating are investigated by a kinetic macroparticle simulation. Although the parameters of kinetic simulation cannot quantitatively match those of experiment and MHD simulation, similar behavior is reproduced. As noted above, the dynamics in the appropriate θ-z plane is essentially $2\frac{1}{2}$D (i.e., the morphology depends on 2D in this plane, while the vectors can be pointed not only in the plane but also normal to this). This electromagnetic macroparticle simulation scheme described in Ref. [19] includes both ion and

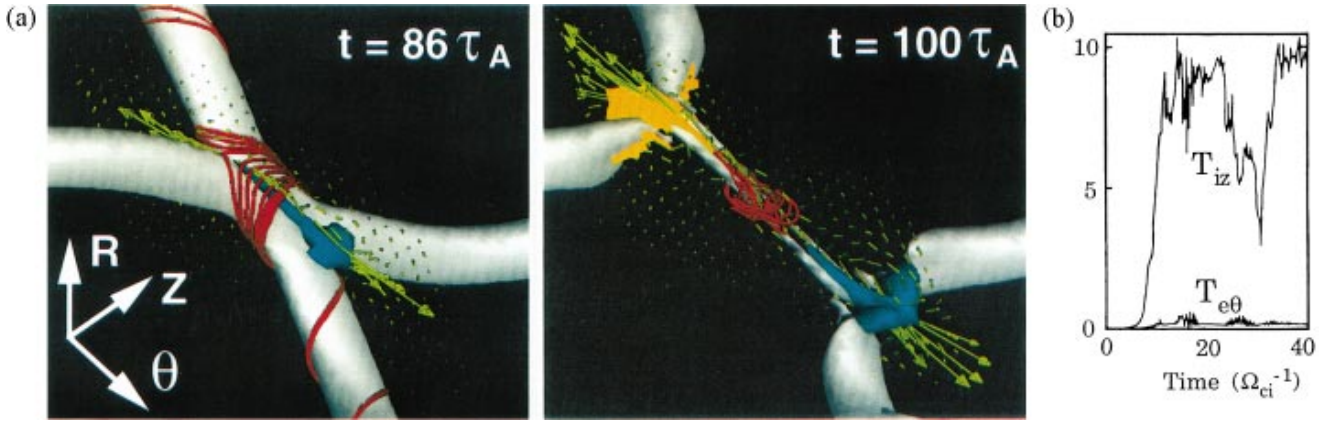

FIG. 3. (a) The result of 3D MHD simulation of the reconnection between counterhelicity flux tubes. The white surfaces show the isosurface of magnetic field strength. The blue and orange surfaces show the isosurfaces of positive and negative toroidal velocities ($v_t = \pm 0.3 v_A$), respectively. The green arrows show vecolity vectors. The red curves are magnetic field lines $t = 86\tau_A$ and $t = 100\tau_A$. (b) The result of $2\frac{1}{2}$D EM (electromagnetic) kinetic macro-particle simulation of counterhelicity coalescence; ion temperauter in the z (colescing) direction and electron temperature in the θ direction.

electron dynamics, allowing for finite Larmor radius effects and charge separation effects. The realized reconnection is basically collisionless ($R_m > 10^4$), but may not be so highly collisionless as that in the magnetosphere, because some screened Coulomb collisions remain. We simulated $2\frac{1}{2}$D coalescing flux tubes where two tubes straight in the θ direction merge together in the z direction without a magnetic field normal to the plane, thus causing a 180° reconnection [8]. This setup is the same as in Ref. [8]. Under this condition, magnetic fields exhibit slingshot oscillations (not shown here) after reconnection. Figure 3(b) shows the time history of ion energy in the coalescing direction (z) and electron energy in the θ direction. (Since electrons are magnetized, their energy in the z direction does not exhibit strong bulk heating, as seen in ions.) Where no magnetic field exists in the counterhelicity case, coalescing flows of ions interpenetrate each other and rapidly mix. This is one major process of ion momentum transfer through ion viscosity. Electrons cannot freely mix and thus no bulk heating of electrons results as they are still magnetized and move through the $\mathbf{E} \times \mathbf{B}$ motion. Since the region that is encircled by the new poloidal fields and does not contain much field inside is substantial (not just the X point or X line), so this interpenetrating ion momentum transfer takes place over a substantial finite volume. This is the most probable reason why the dissipated toroidal magnetic energy is transformed mostly to ions and not to electrons, in agreement with the experiment mentioned.

In summary, a series of experiments and simulations elucidates the ion acceleration and direct ion heating effects in three-component reconnection. Their two important aspects are consistently observed: contraction of reconnected field lines accelerates plasma ions toroidally up to the order of the Alfvén velocity, producing a large velocity shear, and, at the same time, this acceleration process heats plasma ions directly and selectively, converting the dissipated magnetic energy mostly into the ion thermal energy. The ion velocity shear appears in the presence of a large viscosity force because ions are unmagnetized in a wide region where the counterhelicity reconnection annihilates the toroidal field. The work done against this viscosity force is transformed into the ion thermal energy. This heating effect is very small for magnetized electrons, leading to a possible explanation for the $T_i \gg T_e$ characteristics observed in our result. This bulk heating mechanism may give an additional factor in explaining coronal heating whose power is much larger than sheet current dissipation. The observed selective ion heating is also consistent with the RFP experiments whose reconnection has field-line-merging angles as large as 180°.

We would like to thank Dr. R. Kulsrud, Dr. M. Katsurai, and the TS-3 group for useful discussions.

*Present address: Princeton Plasma Physics Laboratory, Princeton University, Princeton, NJ 08543.
†Present address: Chiba University, Chiba, Japan.

[1] S. Tsuneta *et al.*, Publ. Astron. Soc. Jpn. **44**, L63 (1992); K. Shibata *et al., ibid.* **44**, L173 (1992).
[2] E. N. Parker, J. Geophys. Res. **62**, 509 (1957).
[3] H. E. Petschek, in *Proceedings of the AAS-NASA Symposium on the Physics of Solar Flares, Greenbelt, MD, 1963* (U.S. G.P.O., Washington, D.C., 1964), p. 425.
[4] D. Biskamp, Phys. Fluids **29**, 1520 (1986).
[5] E. R. Priest and L. C. Lee, J. Plasma Phys. **44**, 337 (1991).
[6] L. C. Lee and Z. F. Zu, J. Geophys. Res. **91**, 6807 (1992).
[7] K. Shindler and J. Birn, J. Geophys. Res. **92**, 95 (1987).
[8] T. Tajima and J.-I. Sakai, Sov. J. Plasma Phys. **15**, 519 (1989); J. N. Leboeuf *et al.*, Phys. Fluids **25**, 784 (1982).
[9] G. R. Burkhart *et al.*, J. Geophys. Res. **95**, 18 833 (1990).
[10] R. W. Moses *et al.*, J. Geophys. Res. **98**, 4013 (1993).
[11] R. Stenzel *et al.*, J. Geophys. Res. **87**, 111 (1982); W. Gekelman and H. Pfister, Phys. Fluids **31**, 2017 (1988).
[12] K. F. Schenberg *et al.*, in *Proceedings of the 12th International Conference on Plasma Physics and Controlled Nuclear Fusion Research, Nice, France, 1988* (IAEA, Vienna, 1989), Vol. 2, p. 419; E. Scime *et al.*, Phys. Fluids **4**, 4062 (1992).
[13] J. C. Fernandez *et al.*, Nucl. Fusion **30**, 67 (1990); M. Yamada *et al.*, Phys. Fluids **B2**, 3074 (1990).
[14] M. Yamada *et al.*, Phys. Rev. Lett. **65**, 721 (1990).
[15] Y. Ono *et al.*, Phys. Fluids B **5**, 3691 (1993).
[16] Y. Ono *et al.*, in *Proceedings of the 14th International Conference on Plasma Physics and Controlled Nuclear Fusion Research, Würzburg, Germany, 1992* (IAEA, Vienna, 1993), Vol. 2, p. 619; Trans. Fusion Technol. **27**, (1995).
[17] E. Rubin and S. Z. Burstein, J. Comput. Phys. **2**, 17 (1967).
[18] R. O. Richtmyer and K. W. Morton, *Differential Methods for Initial Value Problems* (Interscience, New York, 1967), 2nd ed., Chap. 13.
[19] C. K. Birsall *et al.*, in *Methods in Computational Physics*, edited by B. Alder *et al.* (Academic Press, New York, 1970), Vol. 9, p. 241.